

Published in final edited form as:

*Cell*. 2005 October 21; 123(2): 347–358.

## The Homeodomain Transcription Factor *Irx5* Establishes the Mouse Cardiac Ventricular Repolarization Gradient

Danny L. Costantini<sup>1,2,4,5</sup>, Eric P. Arruda<sup>1,2,4,6</sup>, Pooja Agarwal<sup>1,2,4,6,15</sup>, Kyoung-Han Kim<sup>4,5</sup>, Yonghong Zhu<sup>1,4</sup>, Wei Zhu<sup>1</sup>, Melanie Lebel<sup>2,6</sup>, Chi Wa Cheng<sup>2,10</sup>, Chong Y. Park<sup>11,16</sup>, Stephanie A. Pierce<sup>11</sup>, Alejandra Guerchicoff<sup>12</sup>, Guido D. Pollevick<sup>12</sup>, Toby Y. Chan<sup>13</sup>, M. Golam Kabir<sup>4,13</sup>, Shuk Han Cheng<sup>10</sup>, Mansoor Husain<sup>4,5,7,9,13</sup>, Charles Antzelevitch<sup>12</sup>, Deepak Srivastava<sup>11,16</sup>, Gil J. Gross<sup>1,3,4,8</sup>, Chi-chung Hui<sup>2,6</sup>, Peter H. Backx<sup>4,5,7,14,\*</sup>, and Benoit G. Bruneau<sup>1,2,4,6,\*</sup>

<sup>1</sup>Program in Cardiovascular Research

<sup>2</sup>Program in Developmental Biology

<sup>3</sup>Cardiology Division The Hospital for Sick Children Toronto, Ontario M5G 1X8 Canada

<sup>4</sup>The Heart and Stroke/Richard Lewar Centre of Excellence

<sup>5</sup>Department of Physiology

<sup>6</sup>Department of Molecular and Medical Genetics

<sup>7</sup>Department of Medicine

<sup>8</sup>Department of Pediatrics

<sup>9</sup>McLaughlin Centre for Molecular Medicine, University of Toronto, Toronto, Ontario M5S 1A8, Canada

<sup>10</sup>Department of Biology and Chemistry, City University of Hong Kong, Hong Kong, China

<sup>11</sup>Departments of Pediatrics and Molecular Biology, University of Texas Southwestern Medical Center at Dallas, Dallas, Texas 75390

<sup>12</sup>Masonic Medical Research Laboratory, Utica, New York 13501

<sup>13</sup>Division of Cellular and Molecular Biology, The Toronto General Hospital Research Institute, Toronto, Ontario M5G 2C4, Canada

<sup>14</sup>Division of Cardiology, University Health Network, Toronto, Ontario M5G 2C4, Canada

### Summary

Rhythmic cardiac contractions depend on the organized propagation of depolarizing and repolarizing wavefronts. Repolarization is spatially heterogeneous and depends largely on gradients of potassium currents. Gradient disruption in heart disease may underlie susceptibility to fatal arrhythmias, but it is not known how this gradient is established. We show that, in mice lacking the homeodomain transcription factor *Irx5*, the cardiac repolarization gradient is abolished due to increased  $K_v4.2$  potassium-channel expression in endocardial myocardium, resulting in a selective increase of the major cardiac repolarization current,  $I_{to,f}$ , and increased susceptibility to arrhythmias. Myocardial *Irx5* is expressed in a gradient opposite that of  $K_v4.2$ , and *Irx5* represses  $K_v4.2$  expression by recruiting mBop, a cardiac transcriptional repressor. Thus, an *Irx5* repressor gradient negatively

\*Correspondence: p.backx@utoronto.ca (P.H.B.); bbruneau@sickkids.ca (B.G.B.).

<sup>15</sup>Present address: Cardiovascular Research Institute, University of California, San Francisco, California 94143.

<sup>16</sup>Present address: Gladstone Institute of Cardiovascular Disease, San Francisco, California 94158.

regulates potassium-channel-gene expression in the heart, forming an inverse  $I_{to,f}$  gradient that ensures coordinated cardiac repolarization while also preventing arrhythmias.

## Introduction

Patterning of cardiac-gene expression underlies normal heart development. For example, longitudinal patterning along the anteroposterior axis of the heart establishes the distinctions between atrial and ventricular chambers, while concentric patterning within chambers establishes transmural cardiac growth and gene-expression gradients (Bruneau, 2002; Habets et al., 2003). An important gene-expression gradient is that which defines the cardiac repolarization gradient (Antzelevitch, 2004; Nerbonne and Guo, 2002; Oudit et al., 2001). Following depolarization and ventricular contraction, repolarization initiates cardiac relaxation. In all mammals, ventricular repolarization proceeds in a synchronized wave advancing from the base of the heart to its apex and from epicardial to endocardial myocardium, which is believed to ensure efficient pump function and maintain an arrhythmia-free heart. However, neither how the repolarization gradient is established nor its precise role in modulating the incidence of arrhythmias is known.

For the orderly sequence of repolarization to occur, endocardial myocytes must have longer action-potential durations (APDs) than epicardial cardiac myocytes. This is primarily achieved through differences in the rates of repolarization, and, in several mammalian species, this is linked to regional differences in density of the fast component of the transient outward current,  $I_{to,f}$  (Nerbonne and Guo, 2002; Oudit et al., 2001). The highest density of  $I_{to,f}$  is seen in epicardial myocytes, whereas the lowest density is observed in endocardial myocytes (Figure 1).  $I_{to,f}$  is formed by the heterotetrameric assembly of pore-forming  $\alpha$  subunits,  $K_v4.2$  and  $K_v4.3$ , in association with accessory ( $\beta$ ) subunits such as KChIP2 or frequenin/NCS-1 (Brunet et al., 2004; Guo et al., 2002b; Shibata et al., 2003). In small rodents such as mice and rats, regional heterogeneity of  $I_{to,f}$  in ventricles parallels that of  $K_v4.2$  (Brunet et al., 2004; Guo et al., 2002a; Wickenden et al., 1999a) and possibly  $K_v4.3$  (Kapielian et al., 2002; Wickenden et al., 1999a). In larger mammals such as human and dog,  $K_v4.3$  is the predominant  $I_{to,f}$ -encoding  $\alpha$  subunit in the heart (Nerbonne and Guo, 2002; Oudit et al., 2001), and a gradient of KChIP2 may be related to the graded expression of  $I_{to,f}$  (Deschenes et al., 2002; Rosati et al., 2003). These observations suggest that spatial patterning of  $I_{to,f}$  is tightly regulated in mammalian cardiac myocytes. However, very little is known about the transcriptional regulation of the  $I_{to,f}$  components.

$I_{to,f}$  downregulation and altered heterogeneity of repolarization are hallmark features of diseased myocardium in humans (Antzelevitch, 2004; Kaab et al., 1998; Nerbonne and Guo, 2002), as well as small-animal models (Kapielian et al., 2002). While increases in the dispersion of repolarization are linked to increased susceptibility to ventricular and atrial fibrillation (Antzelevitch, 2004; Tomaselli and Zipes, 2004), disruption of  $I_{to,f}$  gradients may create substrates for local reentry (Guo et al., 2000; Kuo et al., 2001). For example, mice deficient in  $I_{to}$  due to the loss of KChIP2 or to a dominant-negative  $K_v4.2$  transgene show a complete loss of heterogeneity of repolarization and become susceptible to the induction of polymorphic ventricular tachycardia (Guo et al., 2000; Kuo et al., 2001), although loss of current does not directly prove a requirement for a current gradient per se. Since ventricular tachycardia can be lethal by directly impairing pump function or by inducing ventricular fibrillation, further understanding the basis for regional heterogeneity of repolarization is clearly of physiological and pathophysiological interest.

Cardiac patterning is accomplished largely via transcription factors expressed in specific compartments of the developing heart (Bruneau, 2002; Habets et al., 2003). The Iroquois

homeobox (*Irx*) genes encode a conserved family of transcription factors that specify the identity of diverse territories of the body in most metazoans by establishing proper spatial and temporal patterns of target genes (Cavodeassi et al., 2001). They encode proteins with a conserved homeodomain of the three-amino acid length extension (TALE) superclass and a conserved 13 amino acid-residue motif, the Iro box, which is unique to the family (Burglin, 1997). Mammalian *Irx* genes show overlapping expression patterns in the developing central nervous system, limbs, heart, and skin, and all six *Irx* genes display specific expression patterns in the developing heart (Bruneau et al., 2000, 2001a; Christoffels et al., 2000; Cohen et al., 2000; Mummenhoff et al., 2001). To date, only *Irx4* has been shown to have a role in heart development (Bao et al., 1999; Bruneau et al., 2001a; Lebel et al., 2003).

In the present study, we show that, in *Irx5*-deficient mice, the cardiac repolarization gradient is flattened due to increased  $K_{v4.2}$  potassium-channel expression in endocardial myocardium, resulting in a selective increase of  $I_{to,f}$  and susceptibility to arrhythmias. Myocardial *Irx5* is expressed in an endocardial-to-epicardial gradient in mouse and dog, and *Irx5* can repress expression of the gene encoding  $K_{v4.2}$  (*Kcnd2*) via recruitment of the cardiac transcriptional repressor mBop. Thus, a repressor gradient of *Irx5* negatively regulates potassium-channel-gene expression in the heart, forming an inverse  $I_{to,f}$  gradient that ensures coordinated cardiac repolarization. This suggests a novel mechanism for the patterning of gene expression in the developing heart and shows a requirement for the cardiac repolarization gradient to reduce the risk of arrhythmia.

## Results

### Electrophysiological Defects in *Irx5*-Deficient Mice

Mice homozygous for a targeted deletion of *Irx5* are viable and fertile but have defects in differentiation of retinal cone bipolar cells and are slightly smaller than their wild-type counterparts (Cheng et al., 2005). To identify a potential role for *Irx5* in cardiac form or function, 8-week-old *Irx5*<sup>+/+</sup>, *Irx5*<sup>+/-</sup>, and *Irx5*<sup>-/-</sup> mice were examined by histology and in vivo echocardiography and hemodynamics, which revealed no abnormalities. However, signal-averaged surface electrocardiography (SAECG, data not shown) and in vivo telemetric electrocardiography in awake, free-moving mice (Figure 2A) revealed that, while heart rate, PR interval, and QRS duration were not affected in *Irx5*<sup>-/-</sup> hearts, there was a significantly decreased amplitude of electrical signals that correlate to ventricular repolarization (Danik et al., 2002; Liu et al., 2004), which we refer to as the T wave. This was apparent on leads I and II of the SAECG. The absolute T wave amplitudes ( $T_{amp}$ ) were measured from the isoelectric point to the most negative point of the T wave, showing that the T wave remained isoelectric in adult *Irx5*<sup>-/-</sup> mice, whereas a pronounced downward T wave deflection was identified in wild-type littermates (Figures 2A and 2B). In the mouse, activation and repolarization follow a pattern similar to that in larger mammals (Liu et al., 2004). The inverted T wave in mice is the summation of vectors reflecting short (8 ms) differences in transmural action-potential durations in the mouse heart (Liu et al., 2004), whereas positive T waves in larger mammals may reflect larger voltage gradients on either side of the M cells during repolarization (Yan and Antzelevitch, 1998). The change in the T wave segment of the ECG suggested a defect in cardiac repolarization in *Irx5*<sup>-/-</sup> mice.

### *Irx5*<sup>-/-</sup> Mice Are Susceptible to Inducible Arrhythmia

Defects in repolarization often result in a predisposition to arrhythmias (Antzelevitch, 2004; Guo et al., 2000; Kuo et al., 2001). As no spontaneous arrhythmias or sudden deaths were observed during 48 hr telemetry recordings, intracardiac programmed stimulation was conducted to determine the susceptibility of *Irx5*<sup>-/-</sup> mice to arrhythmia induction. Ventricular effective refractory periods were shorter in *Irx5*<sup>-/-</sup> mice ( $38 \pm 5$  ms,  $n = 7$ ) compared to wt

mice ( $59 \pm 6$  ms,  $n = 6$ ,  $p < 0.001$ ). Using a protocol in which two to four extra stimuli were applied at the end of a train of eight paced beats to the apex of the right ventricle, ventricular tachycardia (VT) could be reproducibly induced ( $>10$  episodes) in 3 of 7 *Irx5*<sup>-/-</sup> mice but in none of 6 wild-type controls (Figure 2C). In *Irx5*<sup>-/-</sup> mice, induced VTs had a mean length of 21 beats (range 19–30 beats) and duration of 926 ms (range 810–1218 ms). With overdrive pacing, in which continuous rapid pacing is applied, VT was induced in 4 of 7 *Irx5*<sup>-/-</sup> mice, the longest lasting for 180 beats over 14 s (Figure 2D), but in none of the wild-type controls. The propensity for arrhythmias does not seem to correlate with any other measured parameter. Therefore, *Irx5*<sup>-/-</sup> mice are highly susceptible to inducible tachyarrhythmia. Similar to humans with genetic mutations that predispose to arrhythmia in only some cases (Roberts and Brugada, 2003), differences in genetic background or stochastic events may confer arrhythmia inducibility to some *Irx5*<sup>-/-</sup> mice but not others.

### Shorter Action-Potential Duration in *Irx5*<sup>-/-</sup> Endocardial Myocytes

Since alterations in T wave configuration typically reflect regional heterogeneity in the timing of ventricular repolarization, action potentials (APs) were recorded using whole-cell current-clamp techniques in epicardial myocytes isolated from the apical region of the outer left ventricle (LV) free wall or endocardial myocytes isolated from the base of the interventricular septum. As expected, AP durations (APDs) assessed at 25%, 50%, and 90% repolarization (APD<sub>25</sub>, APD<sub>50</sub>, and APD<sub>90</sub>) were longer in endocardial myocytes compared to epicardial myocytes derived from wild-type mice (Figures 3A and 3B). Remarkably, APD<sub>25</sub>, APD<sub>50</sub>, and APD<sub>90</sub> of endocardial myocytes from *Irx5*<sup>-/-</sup> mice were abbreviated compared to wild-type endocardial myocytes ( $p < 0.05$ ) and were not different from those measured in epicardial myocytes from *Irx5*<sup>-/-</sup> or wild-type mice (Figures 3A and 3B). Wild-type and *Irx5*<sup>-/-</sup> myocytes had similar resting membrane potentials and AP amplitudes (data not shown). These results establish that electrical heterogeneity of repolarization is selectively abolished in the *Irx5*<sup>-/-</sup> hearts, consistent with the observed ECG changes.

### Loss of the Ventricular Transmural Gradient of $I_{to}$ in *Irx5*<sup>-/-</sup> Mice

Alterations in repolarization are primarily determined by changes in K<sup>+</sup>-channel expression and function (Nerbonne and Guo, 2002; Oudit et al., 2001). To assess the impact of *Irx5* deficiency on K<sup>+</sup>-current density, whole-cell patch-clamp experiments were conducted on epicardial myocytes from LV apex and endocardial myocytes from the interventricular septal base. Figure 4A shows representative outward K<sup>+</sup>-current waveforms in epicardial and endocardial myocytes isolated from wild-type and *Irx5*<sup>-/-</sup> hearts, with Ca<sup>2+</sup> and Na<sup>+</sup> currents blocked, recorded following depolarizing steps from -40 mV. Corresponding peak current-voltage relationships are shown in Figure 4B. In mouse ventricle, the decaying phase of the outward K<sup>+</sup> currents can be used to identify four overlapping currents with distinct kinetics: rapidly inactivating transient outward K<sup>+</sup> currents ( $I_{to}$ ), two slowly inactivating K<sup>+</sup> currents ( $I_{k,slow1}$  and  $I_{k,slow2}$ ), and sustained noninactivating currents ( $I_{ss}$ ) (Brunet et al., 2004; Xu et al., 1999). As shown in Figure 4C, no measurable differences in densities of  $I_{k,slow1}$ ,  $I_{k,slow2}$ , or  $I_{ss}$  were observed between epicardial and endocardial myocytes in either wild-type or *Irx5*<sup>-/-</sup> mice, demonstrating that these currents do not contribute to differences in APD and repolarization properties (Nerbonne and Guo, 2002; Oudit et al., 2001). On the other hand,  $I_{to}$  density measured following depolarization to +60 mV (Figures 4B and 4C) and maximal  $I_{to}$  conductance ( $G_{to,max}$ , Figure 4D) were greater ( $p < 0.05$ ) in epicardial myocytes than endocardial cells of wild-type mice, consistent with previous work (Brunet et al., 2004; Xu et al., 1999). By contrast,  $I_{to}$  density and  $G_{to,max}$  in endocardial myocytes from *Irx5*<sup>-/-</sup> mice were significantly elevated relative to wild-type endocardial myocytes, resulting in values that were not different from epicardial myocytes from either *Irx5*<sup>-/-</sup> or wild-type hearts (Figures 4B–4D). The  $I_{to}$  gradient was also apparent in myocytes isolated from the epicardial and endocardial layers of the LV free wall, and this gradient was also lost in *Irx5*<sup>-/-</sup> mice (Figure

4F). Therefore, loss of *Irx5* leads to pronounced and specific increases of  $I_{to}$  in the endocardial myocardium, effectively conferring epicardial myocardium properties to the endocardial myocardium.

Despite differences in  $I_{to}$  density and  $G_{to,max}$ , the activation-gating properties of  $I_{to}$  were identical among groups, as assessed from estimates of the voltages required for  $I_{to}$  to reach 50% of the maximal conductance ( $V_{1/2}$ , data not shown). While this suggests that  $I_{to}$  currents are identical between the different groups, previous studies have established that  $I_{to}$  can originate from two distinct currents,  $I_{to,fast}$  ( $I_{to,f}$ ) and  $I_{to,slow}$  ( $I_{to,s}$ ) (Oudit et al., 2001).  $I_{to,f}$  channels are expressed in most myocytes of the LV and recover quickly from inactivation, while  $I_{to,s}$  is found primarily in the ventricular septum and recovers 100-fold more slowly than  $I_{to,f}$  (Brunet et al., 2004; Guo et al., 1999; Xu et al., 1999). To determine whether disruption of the  $I_{to}$  gradient in *Irx5*<sup>-/-</sup> was related to changes in  $I_{to,f}$  or  $I_{to,s}$ , we examined the recovery-from-inactivation properties for  $I_{to}$  (see Figure S1 in the Supplemental Data available with this article online). As expected,  $I_{to}$  recovery in epicardial myocytes was dominated by a similar single rapid component. In endocardial myocytes, recovery of  $I_{to}$  was biphasic, consistent with the existence of both  $I_{to,f}$  and  $I_{to,s}$ . Importantly, the amplitude of the fast component associated with  $I_{to,f}$  was about 2-fold larger ( $p < 0.01$ ) in endocardial myocytes from *Irx5*<sup>-/-</sup> versus wild-type hearts, while the slow  $I_{to,s}$  component was not different (Figure 4E). Time constants were identical in wild-type and *Irx5*<sup>-/-</sup> mice (data not shown). We conclude that *Irx5*<sup>-/-</sup> mice show a selective increase of  $I_{to,f}$  in endocardial myocytes, thus flattening the ventricular repolarization gradient.

#### **K<sub>v</sub>4.2 $\alpha$ Subunits Are Increased in *Irx5*<sup>-/-</sup> Endocardium**

Mouse  $I_{to,f}$  channels reflect the heteromeric assembly of K<sub>v</sub>4.2 and K<sub>v</sub>4.3  $\alpha$  subunits and accessory  $\beta$  subunits such as KChIP2 (Guo et al., 2002a; Shibata et al., 2003). K<sub>v</sub>1.5, in turn, underlies  $I_{k,slow1}$  and has been suggested to demonstrate regional differences in expression in the mouse heart (Brunet et al., 2004; Xu et al., 1999). As expected from the electrophysiological data, K<sub>v</sub>4.2 levels were significantly ( $p < 0.05$ ) higher in epicardial versus endocardial myocardium in wild-type mice and were increased in endocardial myocardium of *Irx5*<sup>-/-</sup> mice, comparable to epicardial levels (Figures 5A and 5B). There were no significant regional differences in the mean relative densities of K<sub>v</sub>4.3 or K<sub>v</sub>1.5 in wild-type or *Irx5*<sup>-/-</sup> hearts (Figures 4A and 4B). There was also a marked increase ( $p < 0.05$ ) in the levels of *Kcnd2* mRNA (encoding K<sub>v</sub>4.2) in *Irx5*<sup>-/-</sup> endocardial myocardium, as well as a slight increase in *Kcna5* mRNA (Figure 4C). These results confirm that K<sub>v</sub>4.2 determines the transmural gradient of  $I_{to,f}$  expression in the mouse heart and demonstrate that transcriptional upregulation of *Kcnd2* in *Irx5*<sup>-/-</sup> mice results in increased expression of K<sub>v</sub>4.2-encoding ion channels and larger density of  $I_{to,f}$  in the endocardial myocardium, thereby eliminating heterogeneity of repolarization.

#### **Inverse Gradients of *Irx5* and K<sub>v</sub>4.2 across the Ventricular Wall**

Transverse sections of E14.5 and E16.5 embryos were incubated with a polyclonal antibody specific to the carboxyl terminus of the *Irx5* peptide sequence. *Irx5* immunoreactivity was clearly evident in the lungs and heart, showing predominant distribution throughout the interventricular septum and endocardial myocardium of the LV (Figures 6A, 6B, 6D, and 6E). *Irx5*<sup>-/-</sup> embryos showed only background staining and autofluorescence from red blood cells (Figures 6C and 6F). In adult ventricular sections, robust expression of *Irx5* was predominantly observed in the septum and endocardial myocardium of the LV in wild-type hearts (Figures 6G, 6I, and 6M). Thus, these results demonstrate a gradient of *Irx5* in the mouse heart, with predominant expression in septum and endocardial myocardium and lower expression in epicardial myocardium. We could not detect an apex-to-base gradient, suggesting that either *Irx5* only regulates transmural gradients or the gradient is too shallow to detect. Western blots

of fractionated proteins from adult mouse hearts confirmed the predominant expression of *Irx5* in endocardial regions and lower expression in epicardial myocardium (Figures 6J and 6K). *Irx5* was detected in fractionated nuclear proteins from isolated ventricular cardiomyocytes (Figure 6J), suggesting that *Irx5* functions directly within cardiac myocytes. As the components of  $I_{to}$ , especially those that form the gradient, are not completely conserved between mouse and larger mammals, we wished to determine whether the gradient of *Irx5* was conserved. *Irx5* mRNA levels in dog myocardium revealed a clear endocardial-to-epicardial gradient of *Irx5* transcript (Figure 6L), similar to that of the mouse.

Parallel tissue sections of adult wild-type and *Irx5*<sup>-/-</sup> ventricles were also stained using an antibody to K<sub>v</sub>4.2. In wild-type hearts, K<sub>v</sub>4.2 immunoreactivity was expressed in a steep gradient across the left ventricular free wall and was of low abundance in the endocardial myocardium and interventricular septum (Figures 6H and 6M). Thus, the expression of K<sub>v</sub>4.2 is a mirror image of *Irx5* protein distribution. Consistent with the Western blot and RT-PCR results, in *Irx5*<sup>-/-</sup> ventricular sections, homogeneous K<sub>v</sub>4.2 immunoreactivity was detected throughout the entire ventricular myocardium, reflecting increased expression in endocardial myocardium (Figure 6M). Therefore, an endocardial-epicardial gradient of *Irx5* inversely correlates with the epicardial-endocardial gradient of K<sub>v</sub>4.2.

### ***Irx5* Represses *Kcnd2*, the Gene Encoding K<sub>v</sub>4.2**

*Irx5* is expressed in cardiac myocytes and therefore may act directly on *Kcnd2* in these cells. *Irx* proteins act mainly as transcriptional repressors (Gomez-Skarmeta et al., 2001; Itoh et al., 2002; Kudoh and Dawid, 2001; Matsumoto et al., 2004) and occasionally as activators (Bao et al., 1999; Matsumoto et al., 2004). Thus, *Irx5* may act to repress *Kcnd2* in endocardial myocytes. To test this possibility, we examine the function of *Irx5* on the rat *Kcnd2* promoter, which shares a high degree of homology with mouse and human *Kcnd2* (Jia and Takimoto, 2003). We cotransfected isolated neonatal mouse cardiomyocytes with *Kcnd2* reporter constructs and with an *Irx5* expression construct. Consistent with the hypothesis that graded levels of *Irx5* regulate the *Kcnd2* gradient, increasing amounts of *Irx5* dose-dependently repressed *Kcnd2-luciferase* activity (Figure 7A). In contrast, *Irx5* activated *Kcnd2-luciferase* in noncardiac COS7 and 10T1/2 cells (Figures 7B and 7D). There is currently no known consensus *Irx* binding site, and therefore we cannot determine whether *Irx5* binds directly or indirectly to the *Kcnd2* promoter. We conclude that *Irx5* can dose-dependently repress the activity of the *Kcnd2* promoter and hypothesized that *Irx5* repressor activity in cardiac myocytes requires a cardiac-specific corepressor protein.

### ***Irx5* Can Interact with mBop, a Cardiac Corepressor, to Repress *Kcnd2***

In a screen to identify cardiac transcription factors that interact with the MYND- and SET-domain muscle-restricted transcriptional repressor mBop (Gottlieb et al., 2002), we identified *Irx4* as a strong interacting partner (C.Y.P. and D.S., unpublished data). Based on the high degree of similarity between *Irx4* and *Irx5*, we hypothesized that *Irx5* would also interact with mBop. Coimmunoprecipitation assays in COS7 cells demonstrated that both *Irx4* and *Irx5* interact with mBop (Figure 7C). Coexpression of mBop in 10T1/2 cells resulted in a marked abrogation of the *Irx5*-dependent activation of *Kcnd2-luciferase* (Figure 7D). As mBop-mediated repression is thought to rely on recruitment of histone deacetylases (HDACs) (Gottlieb et al., 2002), we examined whether the Bop-mediated repressive effect occurred via HDACs by using the HDAC inhibitor trichostatin A (TSA). Addition of TSA relieved the inhibition by mBop of activation by *Irx5* (Figure 7E). Structure-function analysis of *Irx5* (Figures 7F–7H) demonstrated that deletion of the homeodomain (*Irx5*ΔHD) or all residues following the homeodomain (*Irx5*ΔC1) prevented activation by *Irx5*, while removal of the 153 C-terminal residues (*Irx5*ΔC2), which include the conserved Iro box (Burglin, 1997), did not affect activation but prevented repression of activation by mBop. All mutants localized to the

nucleus, although *Irx5* $\Delta$ H nuclear localization was impaired (Figure S2). Consistent with these observations, *mBop* interacted only weakly or not at all with C-terminal-deletion forms of *Irx5* (Figure 7H). Knockdown of *mBop* mRNA by RNA interference in cardiomyocytes slightly decreased expression of *Kcnd2-luciferase* and, importantly, eliminated the ability of exogenous *Irx5* to repress *Kcnd2-luciferase* (Figure 7I), indicating that endogenous *mBop* may be a critical factor for the repressive actions of *Irx5*. These results demonstrate that *Irx5* can repress *Kcnd2*, and this is likely to occur via interaction with *mBop* and the recruitment of HDACs, although other proteins may also be involved in the repressive actions of *Irx5*. This provides a novel mechanism by which *Irx* transcription factors exert repressive effects during development (Figure 7J).

## Discussion

Our results demonstrate that a repressor gradient of *Irx5* is essential for regulating cardiac  $K^+$ -channel-gene expression, forming an inverse  $I_{to,f}$  gradient and ensuring the concordant propagation of repolarization in the ventricular myocardium. These findings demonstrate the importance of an epicardial-to-endocardial repolarization gradient in prevention of potentially lethal ventricular tachycardia. This may have relevance to patients with heart disease associated with gradient disruption, who are recognized as being at high risk of sudden cardiac death.

### *Irx5* and the $I_{to,f}$ Gradient

The electrophysiological composition of the ventricular myocardium is largely heterogeneous due to the expression of distinct cardiac ion channels. Heterologous expression of  $K_{v4.2}$ -,  $K_{v4.3}$ -, and  $K_{v1.4}$ -channel proteins, for example, has been shown to produce currents with biophysical properties resembling, to varying extents,  $I_{to}$  measured in myocytes, indicating that they are likely the primary correlates of cardiac transient outward  $K^+$  currents (Nerbonne and Guo, 2002; Oudit et al., 2001). Manipulating the expression of putative  $K^+$ -channel genes in vivo has also allowed a better understanding of their role in generating contribution to cardiac  $I_{to,f}$  and  $I_{to,s}$ . For example, overexpression of dominant-negative  $K_{v4.2}$   $\alpha$  subunits attenuates  $I_{to,f}$  (Barry et al., 1998; Wickenden et al., 1999b), while the loss of the  $\beta$  subunit KChIP2, which is required for tetrameric channel assembly (Guo et al., 2002a; Shibata et al., 2003), abolishes  $I_{to}$  (Kuo et al., 2001). The present study reveals a substantial increase in the functional expression of  $I_{to,f}$  in endocardial myocytes of *Irx5* $^{-/-}$  mice, in conjunction with a selective and coordinated upregulation of  $K_{v4.2}$  mRNA and protein levels in endocardial myocardium. This provides conclusive evidence that  $K_{v4.2}$  is a major component of mouse  $I_{to,f}$  and that  $K_{v4.2}$  gradients are responsible for the  $I_{to,f}$  gradient in the mouse heart. Since we did not detect regional differences in the levels of other  $K^+$  currents, our findings support the notion that the primary determinant of regional heterogeneity of repolarization and peak outward  $K^+$  currents in mouse ventricular myocytes is the differential expression of  $I_{to,f}$ .

As in mouse, a *Kcnd2* mRNA gradient exists in rat ventricles that parallels the transmural gradient of  $I_{to,f}$  (Wickenden et al., 1999a). However, it should be noted that the formation of the transmural gradient of  $I_{to,f}$  is not entirely conserved between mammals. For example, in contrast to mouse and rat, *Kcnd2* is not expressed in canine or human myocardium (Nerbonne and Guo, 2002; Oudit et al., 2001). Instead, in larger mammals, a transcriptional gradient of *Kcnip2* (encoding KChIP2) across the ventricular wall is thought to be the primary determinant that underlies the transmural gradient of  $I_{to,f}$  expression (Rosati et al., 2003), although whether the *Kcnip2* mRNA gradient is paralleled by a KChIP2 protein gradient has been questioned (Deschenes et al., 2002). Common among mammals, however, is that  $I_{to,f}$  gradients form the basis for the transmural differences in repolarization across the ventricular myocardium. As in mouse, *Irx5* is expressed in a gradient in dog heart, suggesting that it may be a regulator of

repolarization gradients in larger mammals, including humans, perhaps via other genes such as *Kcnip2*.

### An Inverse Repressor Gradient of *Irx5* Patterns the $K_v4.2$ Transmural Gradient by Recruiting mBOP

The graded transmural expression of *Irx5* is necessary for maintaining the  $K_v4.2$  ventricular gradient by suppressing  $K_v4.2$  expression in regions where *Irx5* is highly expressed. Consistent with this hypothesis, *Irx5* dose-dependently inhibited the activity of a *Kcnd2* promoter construct in cardiac myocytes. In contrast to its repressor activity in cardiac myocytes, *Irx5* activated the *Kcnd2* promoter construct in noncardiac cells. Based on these observations, we hypothesized that, in cardiac cells, *Irx5* associates with a corepressor. Indeed, we show that mBop, a cardiac corepressor (Gottlieb et al., 2002), can associate with *Irx5* and repress its activation of *Kcnd2* in noncardiac cells. Furthermore, we show that endogenous mBop is important for the repressive activity of *Irx5* in cardiac myocytes. We propose a model (Figure 7J) whereby *Irx5* acts on the *Kcnd2* promoter and locally suppresses the expression of  $K_v4.2$  by recruiting mBop, which in turn recruits HDACs to repress *Kcnd2* transcription. The graded repressive effects of *Irx5* would therefore be accomplished by shifting the stoichiometry of transcriptional activator and repressor complexes toward a repressive state with increasing amounts of *Irx5*. Together, our findings of an *Irx5* repressor gradient via corepressor recruitment demonstrate a novel mechanism for the formation of cardiac transcriptional gradients.

Other members of the *Iroquois* gene family are expressed in the heart in unique spatiotemporal patterns, and insights into their various roles in tissue specification emphasize their importance for physiological cardiac function. For example, the expression of *Irx4* in both birds and mammals is confined to the ventricles throughout heart development, and gain-of-function and loss-of-function studies demonstrate an essential role for *Irx4* in regulating the expression of genes to maintain the ventricular phenotype, in part via repression (Bao et al., 1999; Bruneau et al., 2000, 2001a). As *Irx4* can also interact with mBop, it is likely that its repressive actions are also mediated by this interaction and that corepressor recruitment is a general feature of gene regulation by *Irx* proteins.

### Clinical Implications of Alteration in the Repolarization Gradient

Arrhythmias are the leading cause of sudden death in patients with heart failure or cardiomyopathies (Tomaselli and Zipes, 2004). Altered patterns of repolarization are important aspects of heart failure that are thought to contribute its arrhythmogenicity (Antzelevitch, 2004; Tomaselli and Zipes, 2004). Genetic diseases affecting the repolarization properties of the heart, such as long and short QT syndrome, are also important causes of sudden death (Roberts and Brugada, 2003). In long QT syndrome (LQTS), increased spatial dispersion of repolarization associated with delayed repolarization provides a substrate for triggered arrhythmia (Antzelevitch, 2004). Similarly, in short QT syndrome (SQTS), accelerated repolarization contributes to the substrate for ventricular tachycardia and sudden death (Extramiana and Antzelevitch, 2004; Gaita et al., 2003). Although an accurate assessment of the QT interval in *Irx5*<sup>-/-</sup> mice was complicated by the absence of a well-defined T wave, loss of *Irx5* yields a remarkable gain of function of  $I_{to,f}$  that reproduces the pathogenesis associated with SQTS.

The repolarization gradient exists in all mammalian species, and therefore must have a critical role in normal heart function. The differential expression of  $I_{to,f}$  across the various cell layers of the heart ensures spatial heterogeneity of APD and refractory periods, thereby synchronizing cardiac repolarization and enhancing electrical stability of the heart (Antzelevitch, 2004; Nerbonne and Guo, 2002). Spatial heterogeneity of repolarization has also been shown to assist

in the synchronization of  $\text{Ca}^{2+}$  release from the sarcoplasmic reticulum, leading to enhanced mechanical stability and pump efficiency (Kaprielian et al., 2002; Sah et al., 2002). Although increased heterogeneity of repolarization has been shown in larger species to be proarrhythmic, in *Irx5*<sup>-/-</sup> mice, the loss of heterogeneity of repolarization results in increased susceptibility to ventricular tachycardia. As the flattened  $I_{\text{to,f}}$  gradient in *Irx5*<sup>-/-</sup> mice is associated with a marked abbreviation of endocardial APD and refractoriness, this may demonstrate the importance of a prolonged refractoriness within the ventricular myocardium, which serves to increase the wavelength (product of refractory period and conduction velocity) of the reentrant wave beyond the path length available in the mouse heart, thus preventing the development of reentry. Indeed, the ready inducibility of life-threatening polymorphic VT/VF in SQTS has been attributed in part to abbreviation of refractoriness of the myocardium (Extramiana and Antzelevitch, 2004). Our results therefore suggest that the loss of the  $\text{K}_{\text{v}4.2}$  gradient results in an arrhythmogenic substrate and thus reveal the importance of the repolarization gradient in maintaining an arrhythmia-free myocardium. Knowledge of the mechanisms regulating repolarization gradients in the mammalian heart represent an important stepping stone toward potential therapies for arrhythmogenic substrates by targeting the *Irx5*/mBop/ $I_{\text{to,f}}$  pathway.

## Conclusions

We have shown that *Irx5* establishes the cardiac repolarization gradient by its repressive actions on the  $\text{K}_{\text{v}4.2}$  potassium-channel gene. The susceptibility to arrhythmias in *Irx5*<sup>-/-</sup> mice provides compelling evidence that the repolarization gradient per se is an important safeguard against reentrant arrhythmias. The gradient of *Irx5* in the mouse heart is analogous to the Brinker (*Brk*) gradient in *Drosophila*, whereby graded levels of the transcriptional repressor *Brk* establish patterned gene expression that serves to transduce the gradient of the morphogen Decapentaplegic (Muller et al., 2003). We propose that the *Irx5* repressor gradient acts via corepressor recruitment, demonstrating a novel mechanism for the formation of cardiac transcriptional gradients.

## Experimental Procedures

### Animals

*Irx5*<sup>+/-</sup> mice, maintained on a mixed CD-1 strain background, were generated as described elsewhere (Cheng et al., 2005) and were intercrossed to generate *Irx5*<sup>-/-</sup> and *Irx5*<sup>+/+</sup> mice. All animals were cared for according to institutional animal-care requirements.

### Physiological Measurements

Echocardiography, in vivo LV physiological measurements, and electrophysiological analysis of adult mice (8 to 12 weeks old) were performed as previously described (Bruneau et al., 2001b; Mungrue et al., 2002). In vivo electrophysiology studies were performed in mice aged 4 to 6 months and anesthetized with sodium pentobarbital (0.033 mg/g i.p.) (Zhu et al., 2003). All studies were performed and analyzed by a blinded operator.

### Myocyte Isolation and Electrophysiology

Ventricular myocytes were dissociated from the ventricular apex and septal base, or from left ventricular free wall epicardium and endocardium, from adult male mice (8 to 12 weeks old) using procedures previously developed to distinguish regional differences in  $\text{K}^{+}$ -current expression (Brunet et al., 2004; Xu et al., 1999). Action potentials and  $\text{K}^{+}$  currents were recorded at room temperature (20°C–23°C) with the whole-cell patch-clamp technique under current-clamp and voltage-clamp mode, respectively (Sun et al., 2004). A modified double-pulse protocol was used to determine the recovery rate of  $I_{\text{to}}$  from steady-state inactivation (Wickenden et al., 1999a). The action potentials and current recordings were analyzed using

pClamp software (Clampfit 9.0, Axon). The decay phase of outward  $K^+$  currents was rigorously fit with a triexponential function to yield estimates of four kinetically distinct  $K^+$  currents ( $I_{to}$ ,  $I_{K,slow1}$ ,  $I_{K,slow2}$ ,  $I_{sus}$ ) using the AMC maximum-likelihood procedure. (Sun et al., 2004). Monoexponential or biexponential fits were used to fit recovery-from-inactivation data (Wickenden et al., 1999a).

### Analysis of mRNA and Protein Levels

RNA was isolated from LV apex and septal base from adult (8- to 11-week-old) mice and epicardial and endocardial sections from the LV of hearts from mongrel dogs (weighing 20–25 kg). Quantitative real-time RT-PCR was performed with assay-on-demand Taq-Man probes (Applied Biosystems): *Kcnd2* (Mm00498065\_m1), *Kcnd3* (Mm00498260\_m1), *Kcna5* (Mm00524346\_s1), *Kcnp2* (Mm000518914\_m1), and *Gapdh* (rodent GAPDH control). Sequences for custom dog *Irx5* Taqman probes were: forward primer, 5'-GCAAGGGCGACTCCGA-3'; reverse primer, 5'-CGCAGCCGC CTTCTG-3'; TaqMan probe, 6-FAM 5'-TCCGCTCCTCCTGCTTC-3'. Western blot analysis was performed on 80 to 100  $\mu$ g of nuclear or membrane protein using rabbit polyclonal anti- $K_v4.2$  (1:200), anti- $K_v4.3$  (1:200), anti- $K_v1.5$  (1:200, all from Chemicon), rabbit anti-mouse GAPDH (1:5000, Amersham Biosciences), or anti-Irx5 antisera (1:1500). Affinity-purified Irx5 antibodies were from rabbit polyclonal antisera raised against the carboxyl terminus of Irx5 fused to GST.

### Immunohistochemistry

Tissues were fixed in 4% paraformaldehyde and embedded in paraffin. For Irx5, sections were incubated with Irx5 antiserum (1:100) overnight at 4°C and then with an anti-rabbit secondary antibody coupled to biotin. For  $K_v4.2$ , the Mouse-On-Mouse kit (Vector) was used. Sections were incubated with monoclonal  $K_v4.2$  antibodies (K57/27, Dr. J. Trimmer) (1:10) overnight with anti-mouse IgG (H+L) secondary antibody coupled to biotin. The Vectastain ABC-AP kit (Vector) and the red substrate kit (Vector) were used to visualize the signal.

### Coimmunoprecipitation and Luciferase Reporter Gene Assays

Transfections of COS7 cells, 10T1/2 cells, or neonatal mouse ventricular myocytes were performed as previously described (Bruneau et al., 2001b), using Fugene6 (Roche) or Lipofectamine 2000 (Invitrogen). Luciferase assays and coimmunoprecipitations were performed as previously described (Bruneau et al., 2001b). mBop siRNA (Dharmacon) sequences were sense 5'-UCACAAGAACGAG UGCGCUTT-3', antisense 5'-AGCGCACUCGUUCUUGUGATT-3'.

### Statistical Analysis

Statistical comparisons were performed by Student's t test or one-way ANOVA.  $p < 0.05$  was considered significant.

### Supplemental Data

Supplemental Data include two figures and can be found with this article online at <http://www.cell.com/cgi/content/full/123/2/347/DC1/>.

### Supplementary Material

Refer to Web version on PubMed Central for supplementary material.

### Acknowledgements

We thank J.N. Wylie for assistance with luciferase assays, K. Takimoto for the *Kcnd2* reporter constructs, and J. Trimmer for  $K_v4.2$  antiserum. This work was supported by grants from the Canadian Institutes of Health Research

(CIHR) to B.G.B., C.-c.H., M.H., and P.H.B.; a CIHR collaborative grant (B.G.B. and M.H.); the NIH/NHLBI (D.S.); and the Research Grants Council of the Hong Kong SAR, China (Project # CityU 1164/02M) to S.H.C., D.L.C. and P.A. were recipients of National Science and Engineering Council of Canada Scholarships, M.L. holds a CIHR Scholarship, and E.P.A. was partly supported by the Hospital for Sick Children Research Training Program. M.H. is a CIHR Clinician-Scientist, M.H. and P.H.B. are Career Investigators of the Heart and Stroke Foundation of Ontario, C.-c.H. is a National Cancer Institute of Canada Scholar, and B.G.B. holds a Canada Research Chair in Developmental Cardiology.

## References

- Antzelevitch C. Cellular basis and mechanism underlying normal and abnormal myocardial repolarization and arrhythmogenesis. *Ann Med* 2004;36 (Suppl 1):5–14. [PubMed: 15176418]
- Bao ZZ, Bruneau BG, Seidman JG, Seidman CE, Cepko CL. *Irx4* regulates chamber-specific gene expression in the developing heart. *Science* 1999;283:1161–1164. [PubMed: 10024241]
- Barry DM, Xu H, Schuessler RB, Nerbonne JM. Functional knockout of the transient outward current, long-QT syndrome, and cardiac remodeling in mice expressing a dominant-negative *Kv4* alpha subunit. *Circ Res* 1998;83:560–567. [PubMed: 9734479]
- Bruneau BG. Transcriptional regulation of vertebrate cardiac morphogenesis. *Circ Res* 2002;90:509–519. [PubMed: 11909814]
- Bruneau BG, Bao ZZ, Tanaka M, Schott JJ, Izumo S, Cepko CL, Seidman JG, Seidman CE. Cardiac expression of the ventricle-specific homeobox gene *Irx4* is modulated by *Nkx2-5* and *dHand*. *Dev Biol* 2000;217:266–277. [PubMed: 10625552]
- Bruneau BG, Bao ZZ, Fatkin D, Xavier-Neto J, Georgakopoulos D, Maguire CT, Berul CI, Kass DA, Kuroski-de Bold ML, de Bold AJ, et al. Cardiomyopathy in *Irx4*-deficient mice is preceded by abnormal ventricular gene expression. *Mol Cell Biol* 2001a;21:1730–1736. [PubMed: 11238910]
- Bruneau BG, Nemer G, Schmitt JP, Charron F, Robitaille L, Caron S, Conner D, Gessler M, Nemer M, Seidman CE, Seidman JG. A murine model of Holt-Oram syndrome defines roles of the T-box transcription factor *Tbx5* in cardiogenesis and disease. *Cell* 2001b;106:709–721. [PubMed: 11572777]
- Brunet S, Aimond F, Guo W, Li H, Eldstrom J, Fedida D, Yamada KA, Nerbonne JM. Heterogeneous expression of repolarizing, voltage-gated  $K^+$  currents in adult mouse ventricles. *J Physiol* 2004;559:103–120. [PubMed: 15194740]
- Burglin TR. Analysis of TALE superclass homeobox genes (*MEIS*, *PBC*, *KNOX*, *Iroquois*, *TGIF*) reveals a novel domain conserved between plants and animals. *Nucleic Acids Res* 1997;25:4173–4180. [PubMed: 9336443]
- Cavodeassi F, Modolell J, Gomez-Skarmeta JL. The *Iroquois* family of genes: from body building to neural patterning. *Development* 2001;128:2847–2855. [PubMed: 11532909]
- Cheng, C.W., Chow, R.L., Lebel, M., Sakuma, R., Cheung, H.O., Thanabalasingham, V., Zhang, X., Bruneau, B.G., Birch, D.G., Hui, C.-c., et al. (2005). The *Iroquois* homeobox gene, *Irx5*, is required for retinal cone bipolar development. *Dev. Biol.*, in press.
- Christoffels VM, Keijsers AG, Houweling AC, Clout DE, Moorman AF. Patterning the embryonic heart: identification of five mouse *Iroquois* homeobox genes in the developing heart. *Dev Biol* 2000;224:263–274. [PubMed: 10926765]
- Cohen DR, Cheng CW, Cheng SH, Hui CC. Expression of two novel mouse *Iroquois* homeobox genes during neurogenesis. *Mech Dev* 2000;91:317–321. [PubMed: 10704856]
- Danik S, Cabo C, Chiello C, Kang S, Wit AL, Coromilas J. Correlation of repolarization of ventricular monophasic action potential with ECG in the murine heart. *Am J Physiol Heart Circ Physiol* 2002;283:H372–H381. [PubMed: 12063311]
- Deschenes I, DiSilvestre D, Juang GJ, Wu RC, An WF, Tomaselli GF. Regulation of *Kv4.3* current by *KChIP2* splice variants: a component of native cardiac *I(to)*? *Circulation* 2002;106:423–429. [PubMed: 12135940]
- Extramiana F, Antzelevitch C. Amplified transmural dispersion of repolarization as the basis for arrhythmogenesis in a canine ventricular-wedge model of short-QT syndrome. *Circulation* 2004;110:3661–3666. [PubMed: 15569843] Published online November 29, 2004. 10.1161/01.CIR.0000143078.48699.0C

- Gaita F, Giustetto C, Bianchi F, Wolpert C, Schimpf R, Riccardi R, Grossi S, Richiardi E, Borggrefe M. Short QT Syndrome: a familial cause of sudden death. *Circulation* 2003;108:965–970. [PubMed: 12925462] Published online August 8, 2003. 10.1161/01.CIR.0000085071.28695.C4
- Gomez-Skarmeta J, de La Calle-Mustienes E, Modolell J. The Wnt-activated Xiro1 gene encodes a repressor that is essential for neural development and downregulates Bmp4. *Development* 2001;128:551–560. [PubMed: 11171338]
- Gottlieb PD, Pierce SA, Sims RJ, Yamagishi H, Weihe EK, Harriss JV, Maika SD, Kuziel WA, King HL, Olson EN, et al. Bop encodes a muscle-restricted protein containing MYND and SET domains and is essential for cardiac differentiation and morphogenesis. *Nat Genet* 2002;31:25–32. [PubMed: 11923873]
- Guo W, Xu H, London B, Nerbonne JM. Molecular basis of transient outward K<sup>+</sup> current diversity in mouse ventricular myocytes. *J Physiol* 1999;521:587–599. [PubMed: 10601491]
- Guo W, Li H, London B, Nerbonne JM. Functional consequences of elimination of i(to,f) and i(to,s): early afterdepolarizations, atrioventricular block, and ventricular arrhythmias in mice lacking Kv1.4 and expressing a dominant-negative Kv4 alpha subunit. *Circ Res* 2000;87:73–79. [PubMed: 10884375]
- Guo W, Li H, Aimond F, Johns DC, Rhodes KJ, Trimmer JS, Nerbonne JM. Role of heteromultimers in the generation of myocardial transient outward K<sup>+</sup> currents. *Circ Res* 2002a;90:586–593. [PubMed: 11909823]
- Guo W, Malin SA, Johns DC, Jeromin A, Nerbonne JM. Modulation of Kv4-encoded K(+) currents in the mammalian myocardium by neuronal calcium sensor-1. *J Biol Chem* 2002b;277:26436–26443. [PubMed: 11994284]
- Habets PE, Moorman AF, Christoffels VM. Regulatory modules in the developing heart. *Cardiovasc Res* 2003;58:246–263. [PubMed: 12757861]
- Itoh M, Kudoh T, Dedekian M, Kim CH, Chitnis AB. A role for iro1 and iro7 in the establishment of an anteroposterior compartment of the ectoderm adjacent to the midbrain-hindbrain boundary. *Development* 2002;129:2317–2327. [PubMed: 11973265]
- Jia Y, Takimoto K. GATA and FOG2 transcription factors differentially regulate the promoter for Kv4.2 K(+) channel gene in cardiac myocytes and PC12 cells. *Cardiovasc Res* 2003;60:278–287. [PubMed: 14613857]
- Kaab S, Dixon J, Duc J, Ashen D, Nabauer M, Beuckelmann DJ, Steinbeck G, McKinnon D, Tomaselli GF. Molecular basis of transient outward potassium current downregulation in human heart failure: a decrease in Kv4.3 mRNA correlates with a reduction in current density. *Circulation* 1998;98:1383–1393. [PubMed: 9760292]
- Kaprielian R, Sah R, Nguyen T, Wickenden AD, Backx PH. Myocardial infarction in rat eliminates regional heterogeneity of AP profiles, I(to) K(+) currents, and [Ca(2+)](i) transients. *Am J Physiol Heart Circ Physiol* 2002;283:H1157–H1168. [PubMed: 12181147]
- Kudoh T, Dawid IB. Role of the iroquois3 homeobox gene in organizer formation. *Proc Natl Acad Sci USA* 2001;98:7852–7857. [PubMed: 11438735]
- Kuo HC, Cheng CF, Clark RB, Lin JJ, Lin JL, Hoshijima M, Nguyen-Tran VT, Gu Y, Ikeda Y, Chu PH, et al. A defect in the Kv channel-interacting protein 2 (KChIP2) gene leads to a complete loss of I(to) and confers susceptibility to ventricular tachycardia. *Cell* 2001;107:801–813. [PubMed: 11747815]
- Lebel M, Agarwal P, Cheng CW, Kabir MG, Chan TY, Thanabalasingham V, Zhang X, Cohen DR, Husain M, Cheng SH, et al. The Iroquois homeobox gene Irx2 is not essential for normal development of the heart and midbrain-hindbrain boundary in mice. *Mol Cell Biol* 2003;23:8216–8225. [PubMed: 14585979]
- Liu G, Iden JB, Kovithavongs K, Gulamhusein R, Duff HJ, Kavanagh KM. In vivo temporal and spatial distribution of depolarization and repolarization and the illusive murine T wave. *J Physiol* 2004;555:267–279. [PubMed: 14634200]
- Matsumoto K, Nishihara S, Kamimura M, Shiraishi T, Otoguro T, Uehara M, Maeda Y, Ogura K, Lumsden A, Ogura T. The prepattern transcription factor Irx2, a target of the FGF8/MAP kinase cascade, is involved in cerebellum formation. *Nat Neurosci* 2004;7:605–612. [PubMed: 15133517]

- Muller B, Hartmann B, Pyrowolakis G, Affolter M, Basler K. Conversion of an extracellular Dpp/BMP morphogen gradient into an inverse transcriptional gradient. *Cell* 2003;113:221–233. [PubMed: 12705870]
- Mummenhoff J, Houweling AC, Peters T, Christoffels VM, Ruther U. Expression of *Irx6* during mouse morphogenesis. *Mech Dev* 2001;103:193–195. [PubMed: 11335133]
- Mungrue IN, Gros R, You X, Pirani A, Azad A, Csont T, Schulz R, Butany J, Stewart DJ, Husain M. Cardiomyocyte overexpression of iNOS in mice results in peroxynitrite generation, heart block, and sudden death. *J Clin Invest* 2002;109:735–743. [PubMed: 11901182]
- Nerbonne JM, Guo W. Heterogeneous expression of voltage-gated potassium channels in the heart: roles in normal excitation and arrhythmias. *J Cardiovasc Electrophysiol* 2002;13:406–409. [PubMed: 12033361]
- Oudit GY, Kassiri Z, Sah R, Ramirez RJ, Zobel C, Backx PH. The molecular physiology of the cardiac transient outward potassium current ( $I_{to}$ ) in normal and diseased myocardium. *J Mol Cell Cardiol* 2001;33:851–872. [PubMed: 11343410]
- Roberts R, Brugada R. Genetics and arrhythmias. *Annu Rev Med* 2003;54:257–267. [PubMed: 12525675]
- Rosati B, Grau F, Rodriguez S, Li H, Nerbonne JM, McKinnon D. Concordant expression of *KChIP2* mRNA, protein and transient outward current throughout the canine ventricle. *J Physiol* 2003;548:815–822. [PubMed: 12598586]
- Sah R, Ramirez RJ, Backx PH. Modulation of  $Ca^{2+}$  release in cardiac myocytes by changes in repolarization rate: role of phase-1 action potential repolarization in excitation-contraction coupling. *Circ Res* 2002;90:165–173. [PubMed: 11834709]
- Shibata R, Misonou H, Campomanes CR, Anderson AE, Schrader LA, Doliveira LC, Carroll KI, Sweatt JD, Rhodes KJ, Trimmer JS. A fundamental role for *KChIPs* in determining the molecular properties and trafficking of *Kv4.2* potassium channels. *J Biol Chem* 2003;278:36445–36454. [PubMed: 12829703]
- Sun H, Oudit GY, Ramirez RJ, Costantini D, Backx PH. The phosphoinositide 3-kinase inhibitor LY294002 enhances cardiac myocyte contractility via a direct inhibition of  $I_{k,s}$  slow currents. *Cardiovasc Res* 2004;62:509–520. [PubMed: 15158143]
- Tomaselli GF, Zipes DP. What causes sudden death in heart failure? *Circ Res* 2004;95:754–763. [PubMed: 15486322]
- Wickenden AD, Jegla TJ, Kapielian R, Backx PH. Regional contributions of *Kv1.4*, *Kv4.2*, and *Kv4.3* to transient outward  $K^+$  current in rat ventricle. *Am J Physiol* 1999a;276:H1599–H1607. [PubMed: 10330244]
- Wickenden AD, Lee P, Sah R, Huang Q, Fishman GI, Backx PH. Targeted expression of a dominant-negative  $K(v)4.2$   $K^+$  channel subunit in the mouse heart. *Circ Res* 1999b;85:1067–1076. [PubMed: 10571538]
- Xu H, Guo W, Nerbonne JM. Four kinetically distinct depolarization-activated  $K^+$  currents in adult mouse ventricular myocytes. *J Gen Physiol* 1999;113:661–678. [PubMed: 10228181]
- Yan GX, Antzelevitch C. Cellular basis for the normal T wave and the electrocardiographic manifestations of the long-QT syndrome. *Circulation* 1998;98:1928–1936. [PubMed: 9799215]
- Zhu W, Lepore JJ, Saba S, Joseph S, Link MS, Homond MK, Estes NAM, Wang PJ, Leiden JM. Cardiac electrophysiologic abnormalities in the *CREBA133* transgenic mouse model of idiopathic dilated cardiomyopathy. *J Cardiovasc Electrophysiol* 2003;14:982–989. [PubMed: 12950544]

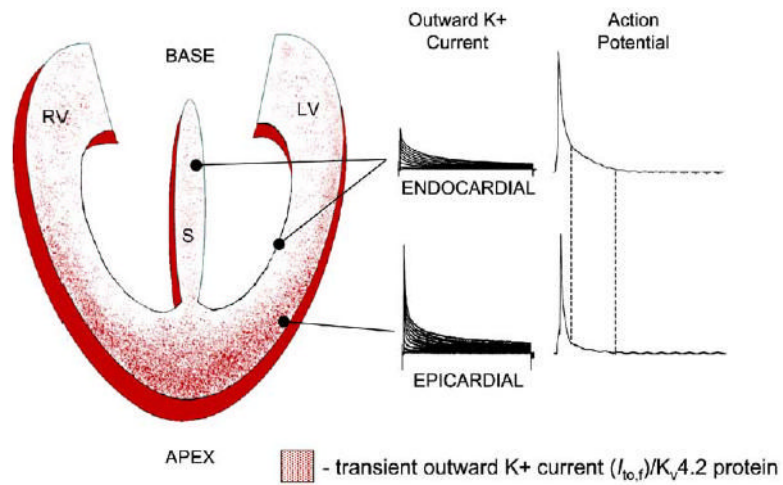


**Figure 1. Repolarization Gradients in the Mammalian Heart**

The gradient of density of  $I_{to,f}$  and K<sub>v</sub>4.2 protein is shown as red dots on a diagram of the heart. Examples of outward currents and action potential resulting from the high  $I_{to,f}$ /K<sub>v</sub>4.2 in epicardial myocardium and low  $I_{to,f}$ /K<sub>v</sub>4.2 in endocardial and septal myocardium are shown. See text for details.

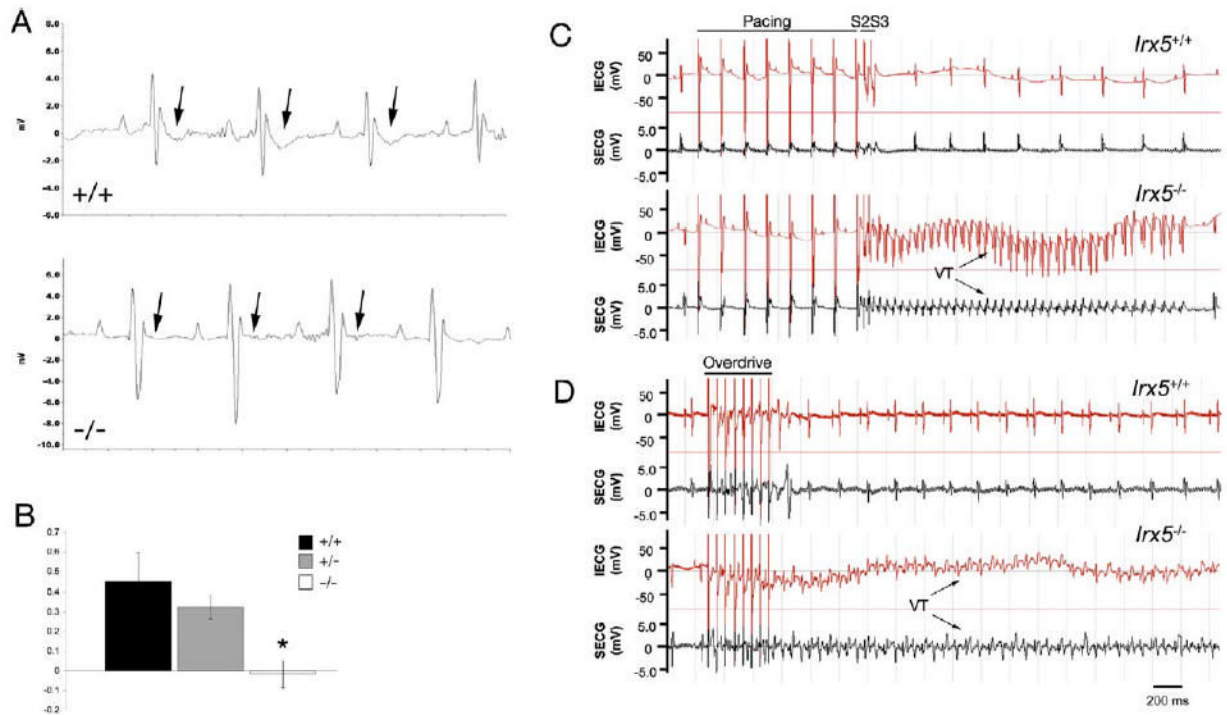


### Figure 2. Absent T Wave and Inducible Arrhythmias in *Irx5*<sup>-/-</sup> Mice

(A) Representative ECGs in the lead II configuration recorded from awake, free-moving mice with the use of telemetric monitoring. Wild-type mice (+/+) show pronounced downward T wave deflections (arrows). No T waves are evident in ECG recordings of *Irx5*<sup>-/-</sup> mice (-/-).

(B) Quantitation of T wave amplitude (mean ± SEM). n = 6–8; \*p < 0.01.

(C and D) Representative intracardiac ECG (IECG, red) and surface ECG (SECG, black) in the lead II configuration obtained from wild-type (*Irx5*<sup>+/+</sup>) and *Irx5*<sup>-/-</sup> mice.

(C) Programmed ventricular stimulation at the right ventricular apex using two extra stimuli (“S2S3”) induced episodes of ventricular tachycardia (VT) in *Irx5*<sup>-/-</sup> mice, whereas no VTs could be induced in wild-type animals.

(D) Rapid overdrive pacing in *Irx5*<sup>-/-</sup> mice also induced VTs of long duration.

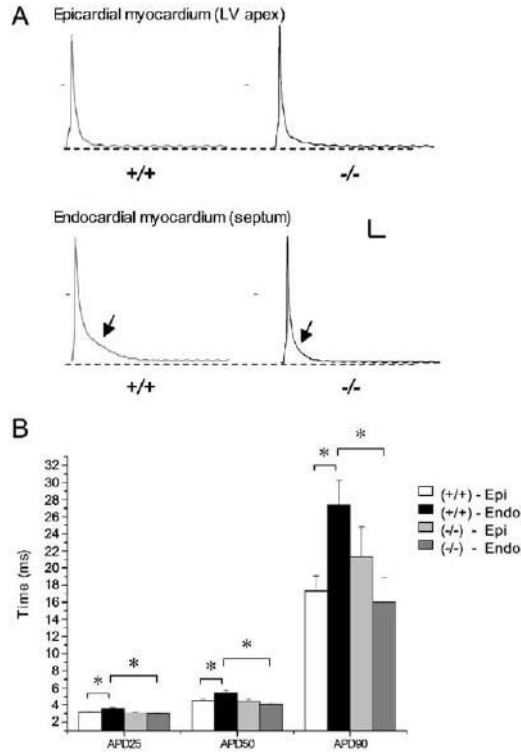


**Figure 3. Shortened Endocardial Action Potentials in *Irx5*<sup>-/-</sup> Cardiomyocytes**

(A) Representative action-potential traces from *Irx5*<sup>+/+</sup> and *Irx5*<sup>-/-</sup> cardiomyocytes from epicardium and endocardium. *Irx5*<sup>-/-</sup> endocardial cardiomyocytes demonstrate a shortening of the action potential (arrows).

(B) Mean action-potential durations (APD) measured at 25%, 50%, and 90% repolarization following complete depolarization. n = 6–14, \*p < 0.05. Scale bars: 20 mV, 25 ms. Data are mean ± SEM.

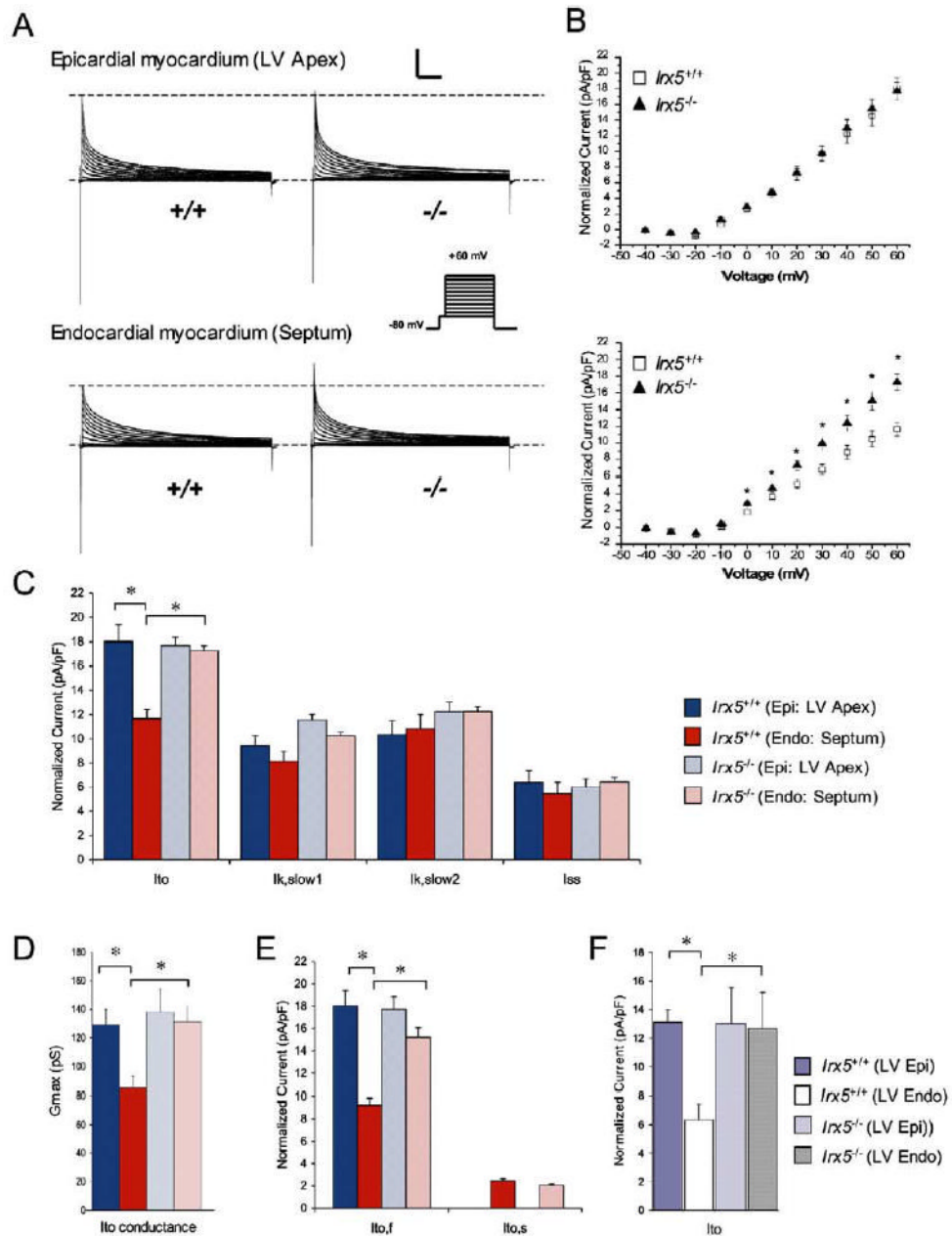


**Figure 4. The Transmural Gradient of *I*<sub>to</sub> Is Eliminated in *Irx5*<sup>-/-</sup> Cardiomyocytes**

(A) Whole-cell outward K<sup>+</sup> currents were recorded from wild-type (+/+) and *Irx5*<sup>-/-</sup> (-/-) cardiomyocytes from epicardial (LV apex) and endocardial (septum) regions of the heart. (B) Mean ± SEM normalized peak *I*<sub>to</sub> amplitudes are plotted as a function of test pulse (top, epicardium; bottom, endocardium). (C) Normalized current densities (pA/pF) for *I*<sub>to</sub>, *I*<sub>k,slow1</sub>, *I*<sub>k,slow2</sub>, and *I*<sub>ss</sub> measured at +60 mV. (D) Maximum current-conductance values for *I*<sub>to</sub> (G<sub>max</sub>). (E) Normalized current densities (pA/pF) for *I*<sub>to,f</sub> and *I*<sub>to,s</sub> measured at +60 mV. (F) Normalized current densities (pA/pF) for *I*<sub>to</sub> measured in myocytes isolated from LV free wall epicardium or endocardium at +60 mV. For all, n = 6–14, \*p < 0.05. Scale bars: 5 nA, 500 ms. Data are mean ± SEM.

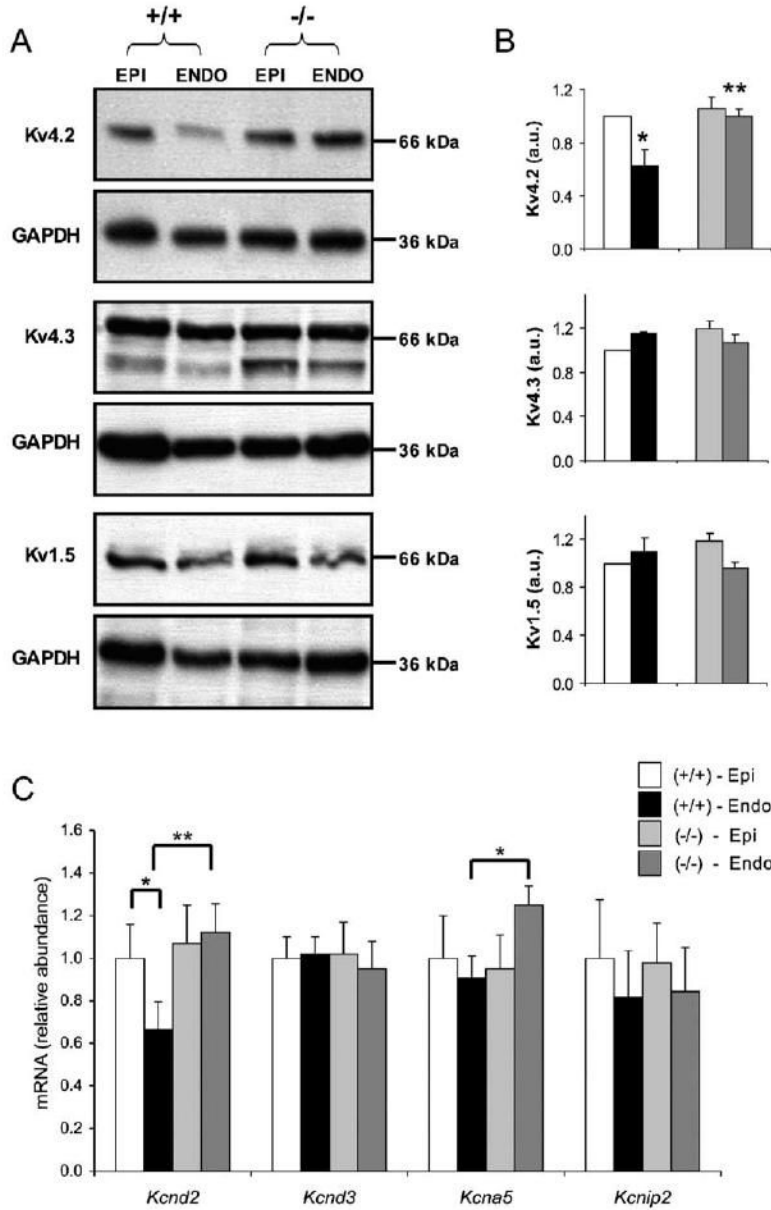


**Figure 5. K<sub>v</sub>4.2 Expression Is Increased in the Endocardium of *Irx5*<sup>-/-</sup> Mice**

(A) Representative Western blots, using specific anti-K<sub>v</sub>4.2, anti-K<sub>v</sub>4.3, and anti-K<sub>v</sub>1.5 antibodies.

(B) Quantitation of Western blot analyses shows increased K<sub>v</sub>4.2 protein in *Irx5*<sup>-/-</sup> endocardial myocardium.

(C) Relative expression of *Kcnd2*, *Kcnd3*, *Kcna5*, and *Kcnip2* in the hearts of wild-type and *Irx5*<sup>-/-</sup> mice assessed by quantitative real-time RT-PCR. mRNA levels (mean ± SEM) are relative to average wild-type epicardial values; n = 6–8, \*p < 0.05 *Irx5*<sup>+/+</sup> endocardial myocardium (Endo) compared with *Irx5*<sup>+/+</sup> epicardial myocardium (Epi), \*\*p < 0.05 *Irx5*<sup>-/-</sup> Endo compared with *Irx5*<sup>+/+</sup> Endo. Data are mean ± SEM.

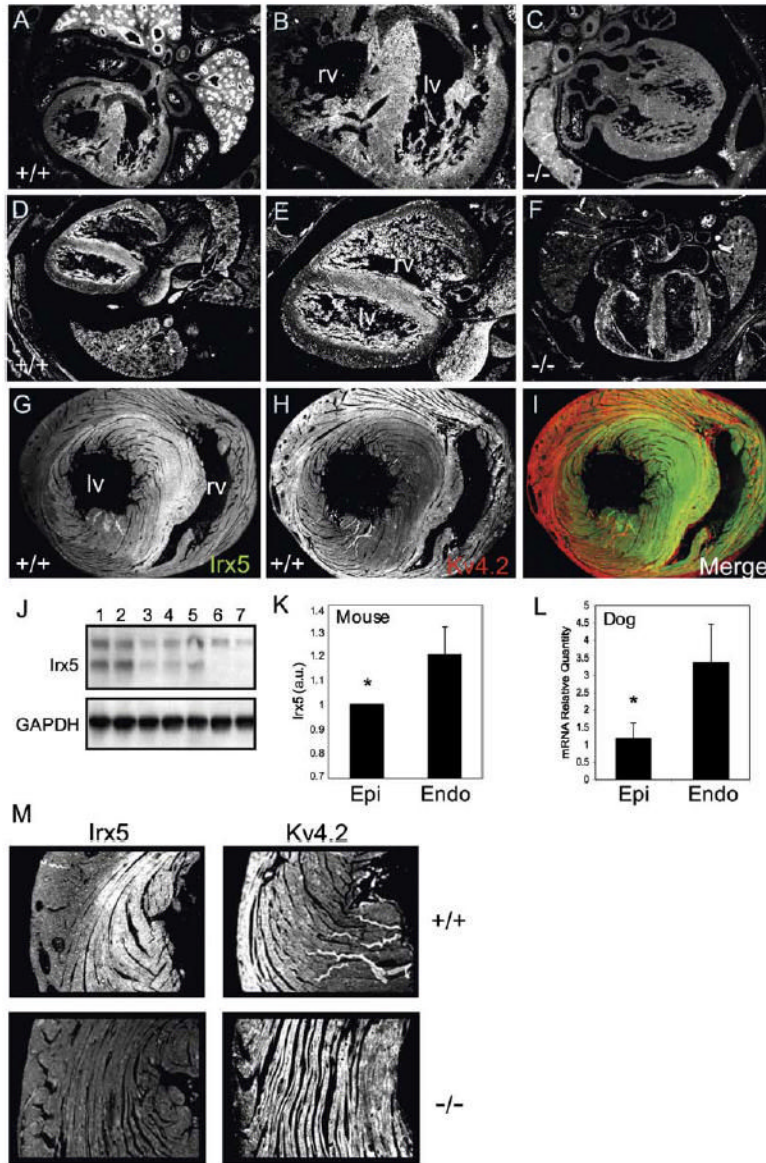


**Figure 6. Inverse Gradients of *Irx5* and *Kv4.2* in the Mouse Heart**

(A–F) Immunohistochemistry for *Irx5* at E14.5 (A and B) and E16.5 (D and E). Regions in (A) and (D) are magnified in (B) and (E). Only background staining is apparent in *Irx5*<sup>-/-</sup> embryos (C and F). lv, left ventricle; rv, right ventricle.

(G and H) *Irx5* (G) and *Kv4.2* (H) expression in adult myocardium.

(I) Images in (G) and (H) were pseudocolored green and red, respectively, and digitally merged.

(J) Western blot showing *Irx5* expression in nuclear extract from epicardial myocardium (lane 1), endocardial myocardium (lane 2), isolated myocytes from epicardial myocardium (lane 3), isolated myocytes from endocardial myocardium (lane 4), isolated neonatal myocytes (lane 5), isolated myocytes from *Irx5*<sup>-/-</sup> epicardial myocardium (lane 6), and isolated myocytes from *Irx5*<sup>-/-</sup> endocardial myocardium (lane 7). GAPDH is shown as loading control.

(K) Quantitation of *Irx5* Western blot; n = 3, \*p < 0.05.

(L) Relative expression of *Irx5* mRNA in dog heart; n = 5, \*p < 0.05. Data are mean ± SEM.

(M) Immunoreactivity of *Irx5* and *Kv4.2* in the ventricles of adult wild-type (+/+) and *Irx5*<sup>-/-</sup> mice (-/-).

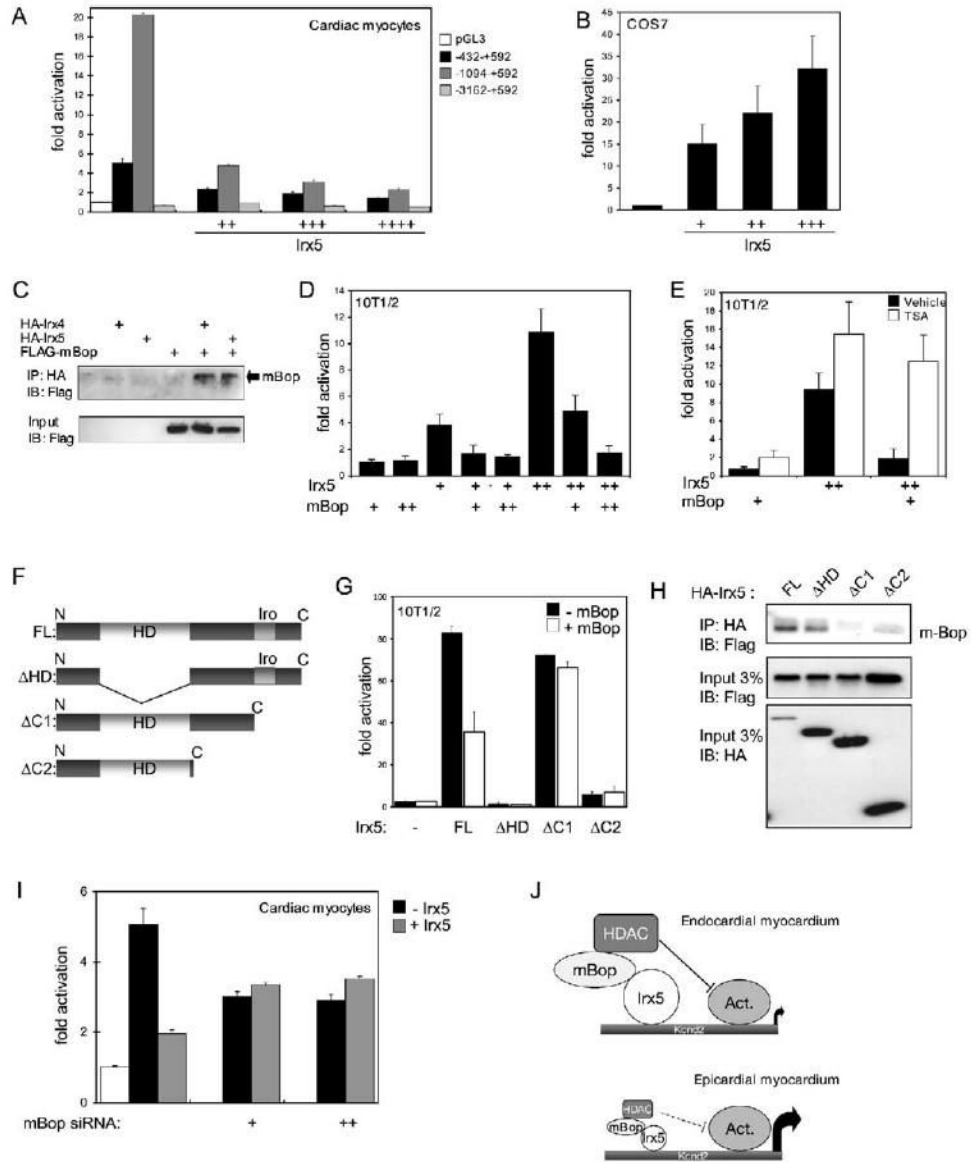


**Figure 7. Irx5 Directly Represses the *Kcnd2* Promoter**

(A) *Kcnd2* -1094+592-luciferase and *Kcnd2* -432+592-luciferase (but not *Kcnd2* -3162+592-luciferase) are strongly activated in neonatal cardiac myocytes. Addition of an Irx5 expression construct (Irx5) reduces the activity of *Kcnd2* reporters. For this and all other panels: +, 100 ng; ++, 250 ng; +++, 500 ng; +++++, 1000 ng Irx5 expression construct.

(B) Irx5 activates *Kcnd2*-luciferase in COS cells.

(C) mBop interacts with Irx4 and Irx5. Immunoprecipitation using anti-HA antibodies followed by immunoblotting against FLAG shows that mBop (arrow) can interact with Irx4 and Irx5.

(D) mBop prevents activation of *Kcnd2* -1094+592-luciferase by Irx5. Similar results were obtained with *Kcnd2* -432+592-luciferase.

(E) Histone deacetylase inhibition by trichostatin A (TSA) relieves the inhibition of Irx5 activity by mBop. In (D) and (E) for mBop: +, 500 ng; ++, 1000 ng expression constructs.

(F) Diagram of Irx5 proteins used in (G) and (H). HD, homeodomain; Iro, Iro box.

(G) *Irx5* $\Delta$ HD or *Irx5* $\Delta$ C2 no longer activates transcription, while *Irx5* $\Delta$ C1 activates but is not repressed by mBop.

(H) Coimmunoprecipitations show that mBop cannot interact with *Irx5* $\Delta$ C1 or *Irx5* $\Delta$ C2.

(I) mBop is required for *Irx5*-mediated repression in cardiac myocytes. siRNAs against mBop (+, 25 ng; ++, 50 ng) reduced expression of *Kcnd2*  $-432$ – $+592$ -*luciferase* and prevented *Irx5*-mediated repression. Data are mean  $\pm$  SEM.

(J) Model for the role of *Irx5*; see text for details.